Molecular Crystals and Liquid Crystals
Publication details, including instructions for authors and subscription information:
http://www.tandfonline.com/loi/gmcl16

Observation of Second Sound Using Light Scattering from a Free Surface Smectic A

M. R. Fisch [a], L. B. Sorensen [a] & P. S. Pershan [a]
[a] Division of Applied Sciences, Harvard University, Cambridge, Massachusetts, 02138, U.S.A.
Version of record first published: 14 Oct 2011.

To cite this article: M. R. Fisch , L. B. Sorensen & P. S. Pershan (1981): Observation of Second Sound Using Light Scattering from a Free Surface Smectic A, Molecular Crystals and Liquid Crystals, 67:1, 165-175

To link to this article: http://dx.doi.org/10.1080/00268948108070885

Mol. Cryst. Liq. Cryst., 1981, Vol. 67, pp. 165–176
0026–8941/81/6704–0165$06.50/0

Observation of Second Sound Using Light Scattering from a Free Surface Smectic A†

M. R. FISCH,‡ L. B. SORENSEN and P. S. PERSHAN

Division of Applied Sciences, Harvard University, Cambridge, Massachusetts, 02138 U.S.A.

(*Received August 5, 1980*)

A new technique for studying the second sound mode in smectic liquid crystals has been developed. Preliminary measurements for the smectic A phase of 4-*n*-octyloxy-4′-cyanobiphenyl (80CB) are described. We have developed a technique to prepare well aligned samples with one free surface. This free surface was electrically driven, and the resulting surface displacement was studied using an optical heterodyne technique. The elastic constant, B, and the effective viscosity, ν_{eff}, were determined from the spectrum of the scattered light.

INTRODUCTION

The experimental measurements that have been made of the smectic elastic constant, B, generally fall into two categories: high frequency measurements of propagating modes and low frequency measurements of overdamped modes. From acoustic experiments at frequencies $\geqslant 1$ MHz, B is obtained from the angular dependence of the quasilongitudinal sound wave.[1] Brillouin scattering extends these measurements to Gigahertz frequencies, and the propagating shear wave that results from non-zero B can *sometimes* be observed.[2,3] Several different light scattering techniques have been used to measure B under conditions in which the shear wave is overdamped. These include both the undulation instability technique[4,5] and correlation time measurements of the intensity of Rayleigh scattered light.[6] In the overdamped

† Work supported by National Science Foundation under Grant No. DMR77-24295 and by the Joint Services Electronics Program (U.S. Army, Navy, and Air Force) under Grant No. N00014-75-C-0648.

‡ Xerox predoctoral fellow.

Paper presented at 8th International Liquid Crystal Conference, Kyoto, Japan, June 30–July 4, 1980.

case the quantity directly measured is the ratio B/K, where K is the Frank constant. There has also been a low frequency propagating mode measurement by Ricard and Prost, who measured B directly by exciting the shear mode with interdigital electrodes.[7]

One of the basic problems in all of these measurements is obtaining well-aligned, defect-free smectic samples. For some geometries this is particularly difficult since undulation instabilities occur spontaneously if the samples are slightly strained, either mechanically or due to thermal effects.

We have developed a new low frequency technique for measuring B directly on samples whose upper surface is a gas–liquid crystal interface. The material parameters of the liquid crystal are determined from the measured spectral distribution of light scattered by the surface displacements. The technique is analogous to measurements of capillary waves on free surface nematics. In contrast to nematic and isotropic samples where the surface displacements are dominated by surface tension, the surface displacements we have measured in smectic samples are dominated by the bulk elastic shear waves. Since the free surface sample should have fewer defects than a confined sample,[8] artifacts originating from sample imperfections should be significantly reduced.

In this paper we shall present a brief summary of the theoretical and experimental aspects of this technique.

THEORETICAL PREDICTIONS

The geometry of our experiment is illustrated schematically in Figure 1. The smectic liquid crystal is supported on a flat rigid surface, so that the top surface is just an air–smectic interface (we describe how such a sample is realized in the next section). The sound modes in this configuration can be obtained by simultaneously solving the hydrodynamic equations for the longitudinal and shear modes and matching boundary conditions at the top and bottom surfaces. If one specifically considers modes of the form $u(z)$ $\exp(i(\omega t - q_\perp x))$ the problem reduces to solving an ordinary differential equation for $u(z)$. Assuming a perfect sample, with negligible permeation and modes whose frequency $\omega \ll v_0 q_\perp$ where v_0 is the longitudinal sound speed the dispersion relation can be approximated as:[9]

$$i\omega v_{\text{eff}}(q_\perp^4 + q_z^4) + \left(\frac{B}{\rho} q_\perp^2 + \omega^2 + 2i\omega v_{\text{eff}} q_\perp^2\right) q_z^2 + \omega^2 q_\perp^2 \simeq 0 \qquad (1)$$

where $q_\perp$ and q_z are respectively the components of wave vector in the smectic planes and normal to them, v_{eff} is the kinematic viscosity which depends on the angle $\psi = \tan^{-1}(q_\perp/q_z)$, and ρ is the density.

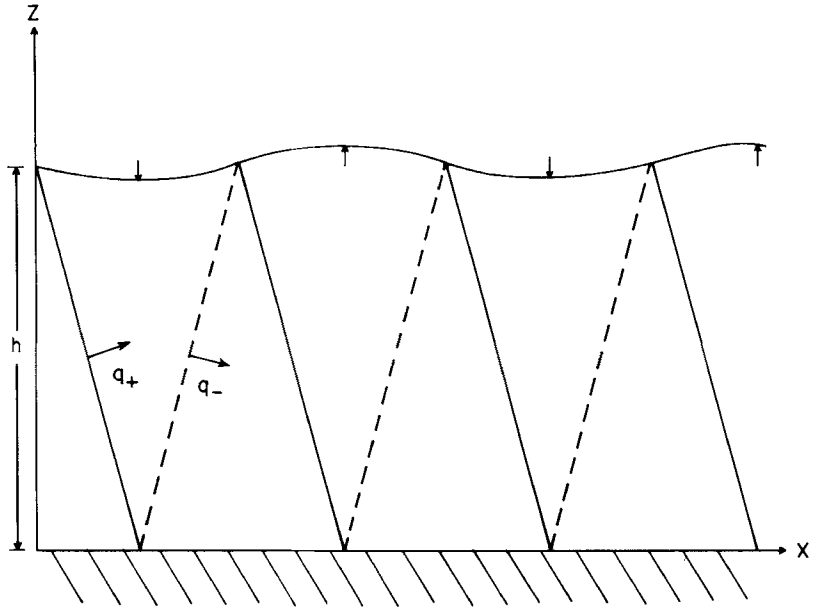

FIGURE 1 The shear wave in a free surface smectic A of height h is shown schematically. The solid lines represent constant phase wavefronts for a wavevector q_+ and the broken lines the wavefronts for q_-. Together these produce zero displacement at the bottom surface and the maximum amplitude for a wave propagating in the x direction at the top surfaces.

Since the dispersion relation is quadratic in q_z^2, there are two roots for q_z^2. The physical significance of these roots is most easily seen in the limit that v_{eff} is infinitesimally small. Then the first solution is just the conventional dispersion relation for second sound in a lossless smectic A:

$$(q_z^a)^2 \approx \frac{\omega^2 q_\perp^2}{\left(\frac{B}{\rho}\right) q_\perp^2 - \omega^2} \tag{2a}$$

or equivalently

$$\omega^2 \approx \left(\frac{B}{\rho}\right) \frac{q_\perp^2 (q_z^a)^2}{q_\perp^2 + (q_z^a)^2}. \tag{2a'}$$

The second solution is infinite if $v_{\text{eff}} = 0$:

$$(q_z^b)^2 = -\frac{i\omega}{v_{\text{eff}}} \frac{q_\perp^2}{(q_z^a)^2}. \tag{2b}$$

The solution with this z dependence describes a boundary layer of thickness $\xi \sim [\text{Real}(q_z^b)]^{-1}$ that is required to match the full boundary conditions. For the typical experimental values of $(B/\rho) \approx 10^7$ (cm/sec)^2, $q_\perp \approx 100\,\text{cm}^{-1}$, $\omega \approx 10^5\ \text{sec}^{-1}$ and $\nu_{\text{eff}} \approx 1\ \text{cm}^2/\text{sec}$, the boundary layer can be neglected (since $\xi \ll h$) and approximate boundary conditions suffice.

The simplest approximation for the boundary conditions of the second sound mode in the free surface geometry are zero stress normal to the free surface and zero displacement at the bottom. This determines a series of normal modes, which for a sample of height, h, have

$$(q_z^a)_n = \frac{\pi}{2h}(2n + 1) \qquad n = 0, 1, 2, \ldots \tag{3}$$

Figure 2 shows the solution to Eq. (1) (including viscous effects, but neglecting boundary layer effects) for the dependence of the second sound frequency on $q_\perp$ for various values of the quantized $(q_z^a)_n$. At large $q_\perp$ the viscous damping causes the solution to become overdamped, and at small $q_\perp$ the boundary layer becomes comparable to the sample thickness. There is, however, a range over which the underdamped propagating modes can exist.

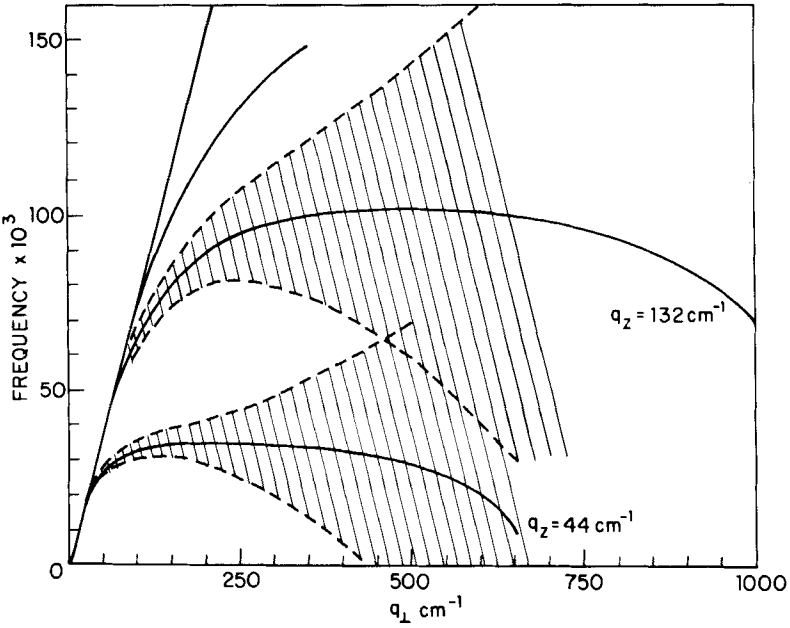

FIGURE 2 The shear wave frequency for a free surface smectic A is shown as a function of $q_\perp$ for a sample of height 360μ with $B/\rho = 2.5 \times 10^7$ (cm/sec)^2 and $\nu_{\text{eff}} = 1.0\ \text{cm}^2/\text{sec}$. The solid lines represent the center frequencies of the modes and the dotted lines indicate the half power frequencies.

The solution shown in Figure 2 is not the correct solution when $\omega/vq^2 \ll 1$. In this regime, the Frank constant term must be kept and the solution is identical to that of the Orsay Group:[10]

$$iq_z = \sqrt{\frac{K}{B}}\, q_\perp^2 \sqrt{1 + \frac{i\omega\rho v_{\text{eff}}}{Kq_\perp^2}} \tag{4}$$

This mode is centered at zero frequency and has a width of $\leqslant 1$ Hz. The amplitude of this mode is approximately two orders of magnitude larger than the propagating smectic wave.

The motion of the free surface of the sample (neglecting permeation, dislocations, etc.) is determined by the hydrodynamics of the smectic layers. Thus the solution to the hydrodynamic equations can be used to compute both the thermally excited surface displacements and the response of the surface to an externally applied force.

To calculate the thermally excited displacements consider a semi-infinite smectic A sample. For the Fourier component

$$u(\mathbf{q}, \omega) = \iint \exp[-i(\omega t - \mathbf{q} \cdot \mathbf{r})] u(\mathbf{r}, t)\, dt\, d\mathbf{r} \tag{5}$$

the spectral density is given by

$$S_{uu}(\mathbf{q}, \omega) = \frac{2k_B T v_{\text{eff}} q^2}{\rho[(\omega^2 - \omega_0^2) + \omega^2 v_{\text{eff}} q^4]} \tag{6}$$

where

$$\omega_0^2 = \frac{B}{\rho} \frac{q_\perp (q_z^a)^2}{q_\perp^2 + (q_z^a)^2} + \frac{K}{\rho} \frac{q_\perp^6}{q_\perp^2 + (q_z^a)^2},$$

k_B is Boltzmann's constant and T is the absolute temperature. The thermal mean square deviation in the layer displacement is given by

$$\langle u(q)^2 \rangle = \frac{1}{2\pi} \int S_{uu}(q, \omega)\, d\omega = \frac{k_B T}{\omega_0^2 \rho}. \tag{7}$$

For the typical experimental values of $(B/\rho) \approx 10^7$ (cm/sec)^2, $q_\perp = 125$ cm^{-1}, $(q_z^a)_0 \approx 100$ cm^{-1} and $T \approx 300$ K this becomes

$$\langle u(q)^2 \rangle = 7 \times 10^{-25} \text{ cm}^2 \tag{8}$$

Although the system described in the next section is very sensitive ($\sim 10^{-20}$ cm^2/sec scan), the thermally excited modes are so weak that it is impractical to study them directly.

It is possible, however, to externally drive the surface of the sample at a single frequency and to produce surface displacements with much greater amplitudes than the thermally excited displacements. In this case the

response is given by the sum of the responses of each mode

$$u = \sum_n u_n = \sum_n \frac{(\omega_n^2 - \omega^2) - i\gamma\omega}{(\omega_n^2 - \omega^2)^2 + \gamma^2\omega^2} F_0 e^{i\omega t} \tag{9}$$

where

$$\omega_n^2 = \frac{B}{\rho}\left[\frac{q_\perp^2 (q_z^a)_n^2}{q_\perp^2 + (q_z^a)_n^2}\right]$$

and

$$\gamma = v_{\text{eff}}[q_\perp^2 + (q_z^a)_n^2].$$

The predicted response for typical material and experimental parameters is shown in Figure 3. The responses corresponding to $n = 0$, $n = 1$ and $n = 2$ are clearly visible. For thinner samples the response is dominated by the $n = 0$ mode.

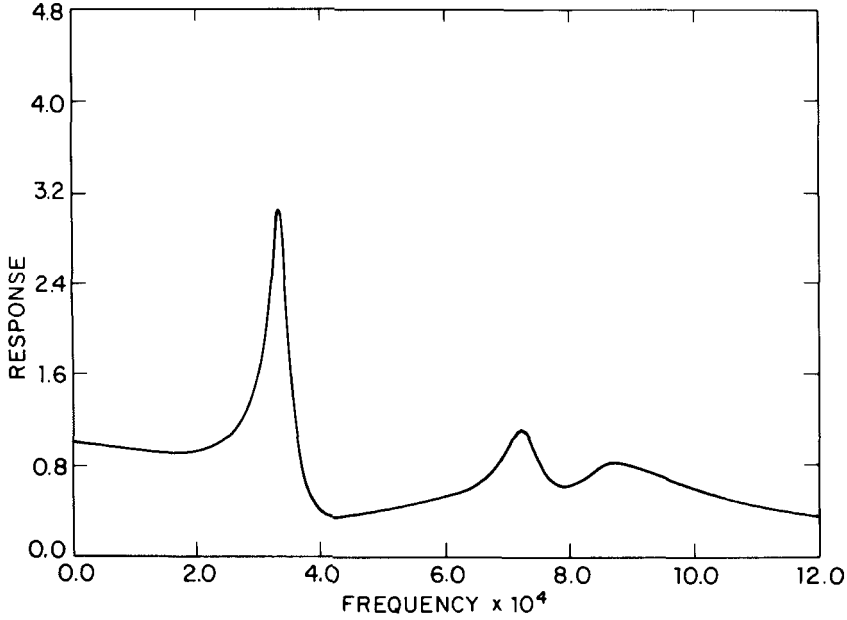

FIGURE 3 The driven frequency response for a free surface sample of height 360μ with $B/\rho = 2.5 \times 10^7$ (cm/sec)^2, $v_{\text{eff}} = 1.0$ cm^2/sec, and $q_\perp = 125$ cm^{-1} calculated from Eq. (9).

EXPERIMENTAL ASPECTS

A Sample preparation

It is commonly believed that it is impossible to prepare free surface smectic liquid crystals that have large areas that are free from Grandjean Terraces. We have developed a simple scheme to greatly reduce the occurrence of these discontinuities in thickness. This scheme is based upon the observation that no meniscus forms when a plate is inserted into a fluid at the contact angle for the fluid, gas, plate system. Our sample cell consists of a tin oxide coated glass flat that is sealed (with indium) to the bottom of a polished brass cell which has sloped sides, (see Figure 4), The cell and the flat are coated with surfactant in order to enhance the homogeneous alignment of the liquid crystal. By varying the angle α one can obtain convex ($\alpha < \alpha$ flat), concave ($\alpha > \alpha$ flat) or flat samples, thereby allowing us to compensate for temperature variations in the surface tension. The contact angle for our cell when filled with 4-*n*-octyloxy-4′-cyanobiphenyl (80CB) is 10.5°. This leads to slightly convex samples in the nematic phase. However, the surface tension in the smectic phase is smaller than in the nematic phase and hence cooling into the smectic phase produces quite flat samples.

The procedure for making samples is rather simple. The oven is heated to a temperature above the nematic–isotropic phase transition, and the liquid crystal is placed on the cell. Special care is taken to ensure that the sides and the flat, are all well coated with liquid crystal. The sample is then slowly cooled into the smectic phase. This usually does not immediately produce a sample of outstanding quality. However, by cycling the sample up to the isotropic phase and back down to the smectic phase several times, excellent alignment is obtained. (See Figure 5.) Conoscopic observations of these samples show well-spaced rings similar to those obtained in confined samples, whereas for samples with even modest height variations the ring spacing becomes noticeably smaller as one looks further from the forward direction. Observations of the well aligned samples with a polarized microscope show a large center area that is free from defects and uniformly grey surrounded by concentric rings of excluded dust near the edges. We believe that these samples are significantly better aligned than confined samples.

B Experimental apparatus

A schematic drawing of the experimental apparatus is shown in Figure 4. It is similar to the system of Hård *et al.*[11] It consists of an Ar^+ laser (~ 200 mW at 5145 Å) weakly focussed onto the sample. A weak diffraction grating is placed after the sample to provide the stable local oscillator of constant

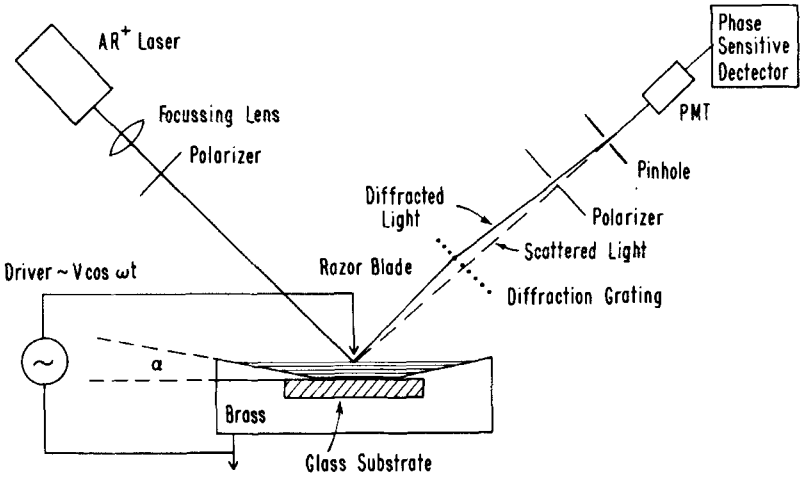

FIGURE 4 Schematic drawing of the experimental set-up and sample cell.

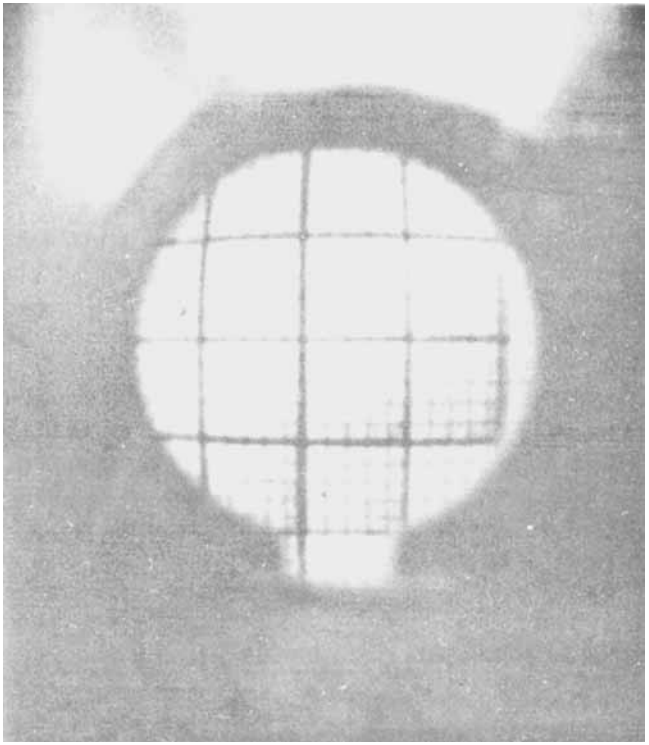

FIGURE 5 Photograph of an $\sim 140\mu$ sample viewed from above. The grid is a piece of graph paper ~ 10 cm under the sample.

scattering vector needed for a heterodyne experiment. The diffraction spots from this grating have a power of $\approx 5 \times 10^{-7}$ watts, and will track any rocking motion of the sample due to extraneous vibrations. One of these spots (corresponding to the desired discrete scattering vector, $q_\perp$) is selected with a pinhole large enough to pass just that *one* spot and the area around it in which it is expected to move. This light then impinges on a photomultiplier (RCA 7265). After amplification it is frequency analyzed with a spectrum analyzer (thermally driven experiment) or a lock-in amplifier (externally driven experiment). This system has excellent immunity to room vibrations and is quite sensitive. A single 4-second scan of a thermally excited nematic surface wave ($u_{\text{rms}} \simeq 10^{-2}$ Å) has a $S/N \simeq 2$. This may be further enhanced by signal averaging. The extremely small amplitude of the smectic waves' surface displacement makes comparable sensitivities necessary.

It was shown in the previous section that the thermally excited smectic bulk waves lead to very small displacements of the liquid crystal surface and hence produce very weak scattered signals. To produce surface displacements with larger amplitudes the surface was driven using the technique developed by Sohl *et al.*[12] for nematic and isotropic samples. A razor blade was placed approximately 50 μ above the surface and an oscillating potential was applied between the razor blade and the tin oxide coating on the glass flat. When the field is applied, the dielectric (liquid crystal) moves into the field until the energy reduction from the dielectric moving into the field is just equal to the increase in the elastic energy of the dielectric. For a peak-to-peak voltage of 50 volts applied to the nematic phase, the amplitude of the Fourier component of the displacement at $q_\perp \approx 125\ \text{cm}^{-1}$ is ≈ 1 Å or roughly one hundred times larger than the thermally excited amplitude. With the present driver it is difficult to excite modes with $q_\perp > 150\ \text{cm}^{-1}$, this sets an upper limit on the $q_\perp$ that can be experimentally observed.

EXPERIMENTAL RESULTS

The driven response of a $\sim 140\ \mu$ thick sample of 80CB is shown in Figure 6 for a $\Delta T = T_{\text{NA}} - T$ of 3.6°C. From the measured S/N ratio we estimate the amplitude of the Fourier component of the surface displacement at $q_\perp \approx 125\ \text{cm}^{-1}$ to be $\sim 10^{-2}$ Å. The solid line through the data represents a rough fit to the theoretical form given by Eq. (9), with the parameter B and v_{eff} varied to obtain a reasonable fit. Figure 7 shows the temperature dependence of B obtained from the data for temperatures far from T_{NA}. Although the simple oven used in these experiments does not allow precise temperature measurements it is clear that B is becoming smaller as $T \to T_{\text{NA}}$. With improved temperature control, it should be possible to measure the critical exponent for B.

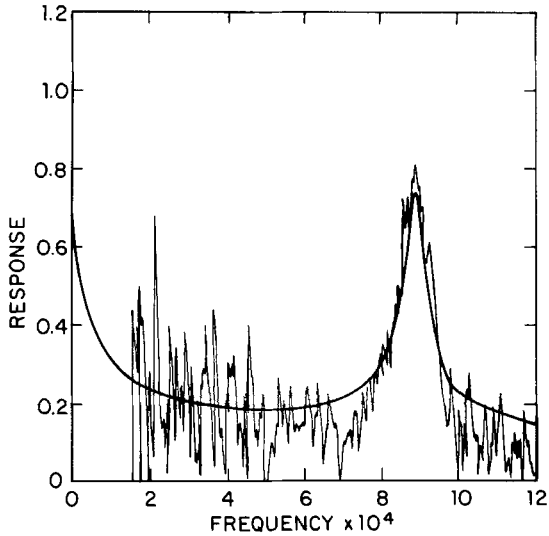

FIGURE 6 The experimental data is shown for $\Delta T = 3.6°C$. The solid line represents a rough fit to the data calculated from eq. (9) with $h = 140\mu$, $B/\rho = 4.4 \times 10^7$ (cm/sec)^2, $\nu_{eff} = 1.1$ cm^2/sec and $q_\perp = 125$ cm^{-1}.

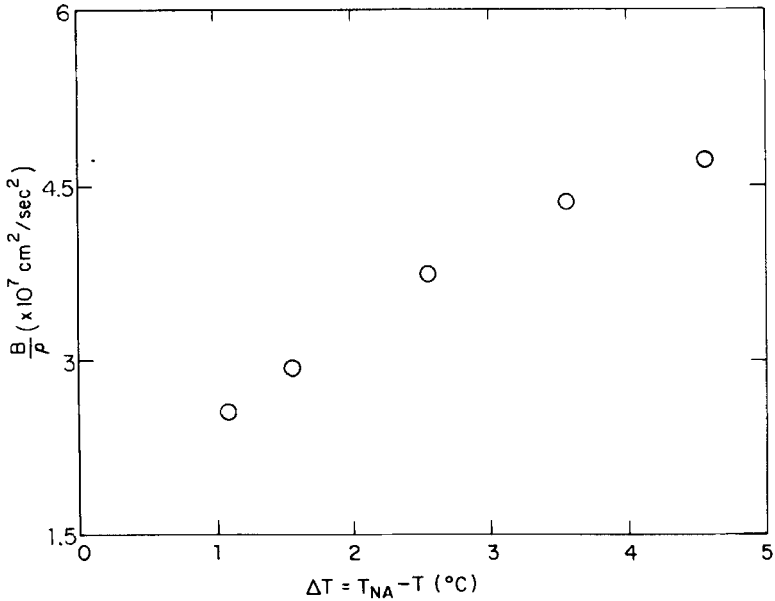

FIGURE 7 The smectic elastic constant, B, is shown as a function of temperature below the nematic-smectic A phase transition. For the simple oven used for these preliminary measurements the uncertainty in ΔT is about 0.3°C.

References

1. K. Miyano and J. B. Ketterson, *Physical Acoustics Principles and Methods, Vol. XIV*, (Academic Press, New York), 1979, p. 93.
2. A. Wergin, W. Krasser, H. H. Stiller, and C. G. B. Frischkorn, *Phys. Rev. A*, **20**, 1120, (1979).
3. Y. Liao, N. A. Clark, and P. S. Pershan, *Phys. Rev. Lett.*, **30**, 639, (1973).
4. N. A. Clark, *Phys. Rev. A*, **14**, 1551, (1976).
5. R. Ribotta, *C.R. Hebd. Séan Acad. Sci.*, **279B**, 295 (1974).
6. H. Birecki, R. Schaetzing, F. Rondelez, and J. D. Litster, *Phys. Rev. Lett.*, **36**, 1376, (1976).
7. L. Ricard and J. Prost, *J. de Phys.*, **40**, C3-83, (1979).
8. P. S. Pershan, *J. Appl. Phys.*, **45**, 1590, (1974).
9. P. C. Martin, O. Parodi, and P. S. Pershan, *Phys. Rev. A*, **6**, 2401, (1972).
10. Orsay Group on Liquid Crystals, *J. de Phys.*, **36**, Supp. C1, 305, (1975).
11. S. Hård, Y. Hamnerius, and O. Nilsson, *J. Appl. Phys.*, **47**, 2433, (1976).
12. C. H. Sohl, K. Miyano, and J. B. Ketterson, *Rev. Sci. Inst.*, **49**, 1464, (1978).